doi:10.1093/brain/awh568 *Brain* (2005), **128,** 2396–2407

Metabolic dysfunction during neuronal activation in the *ex vivo* hippocampus from chronic epileptic rats and humans

Oliver Kann,[1] Richard Kovács,[1,3] Marleisje Njunting,[1,2] Christoph Joseph Behrens,[1] Jakub Otáhal,[1] Thomas-Nicolas Lehmann,[2] Siegrun Gabriel[1] and Uwe Heinemann[1]

[1]Institute for Neurophysiology and [2]Department of Neurosurgery, Charité—Universitätsmedizin Berlin, Germany and [3]Department of Neurochemistry, Institute of Biomolecular Chemistry, Budapest, Hungary

Correspondence to: Dr. med. Oliver Kann, Institut für Neurophysiologie, Charité—Universitätsmedizin Berlin, Tucholskystrasse 2, 10117 Berlin, Germany
E-mail: oliver.kann@charite.de

Metabolic dysfunction has been implicated in the pathogenesis of temporal lobe epilepsy (TLE), but its manifestation during neuronal activation in the *ex vivo* hippocampus from TLE patients has not been shown. We characterized metabolic and mitochondrial functions in acute hippocampal slices from pilocarpine-treated, chronic epileptic rats and from pharmaco-resistant TLE patients. Recordings of NAD(P)H fluorescence indicated the status of cellular energy metabolism, and simultaneous monitoring of extracellular potassium concentration ($[K^+]_o$) allowed us to control the induction of neuronal activation. In control rats, electrical stimulation elicited biphasic NAD(P)H fluorescence transients that were characterized by a brief initial 'drop' and a subsequent prolonged 'overshoot' correlating to enhanced $NAD(P)^+$ reduction. In chronic epileptic rats, overshoots were significantly smaller in area CA1, but not in the subiculum as compared to controls. In TLE patients, who were histopathologically classified in groups with and without Ammon's horn sclerosis (AHS, non-AHS), large drops and very small overshoots of NAD(P)H transients were observed in dentate gyrus, CA3, CA1 and subiculum. Nevertheless, monitoring mitochondrial membrane potential ($\Delta\Psi_m$) by mitochondria-specific, voltage-sensitive dye (rhodamine-123) revealed similar mitochondrial responses during neuronal activation with glutamate and protonophore application in area CA1 of control and chronic-epileptic rats. Applying confocal laser scanning microscopy, these findings were confirmed in individual neurons of AHS tissue, indicating a negative $\Delta\Psi_m$ and activation-dependent mitochondrial depolarization. Our data demonstrate severe metabolic dysfunction during neuronal activation in the hippocampus from chronic epileptic rats and humans, although mitochondria maintain negative $\Delta\Psi_m$. Thus, our findings provide a cellular correlate for 'hypometabolism' as described for epilepsy patients and suggest mitochondrial enzyme defects in TLE.

Keywords: hypometabolism; mitochondria; NADPH; potassium [K]; temporal lobe epilepsy

Abbreviations: $\Delta\Psi_m$ = mitochondrial membrane potential; ACSF = artificial cerebrospinal fluid; AHS = Ammon's horn sclerosis; CCCP = cyanide *m*-chlorophenyl hydrazone; $[K^+]_o$ = extracellular potassium concentration; TLE = temporal lobe epilepsy

Received April 11, 2005. Revised May 15, 2005. Accepted May 19, 2005. Advance Access publication June 15, 2005

Introduction

Temporal lobe epilepsy (TLE) is a prevalent form of focal epilepsy that is frequently resistant to anticonvulsants and, in some patients, progressive in nature (Engel, 2001; Pitkänen and Sutula, 2002). The mechanisms underlying the pathogenesis of TLE remain unclear.

Hippocampal tissue from TLE patients is often characterized by neuronal loss and astrogliosis (Ammon's horn sclerosis, AHS) (Margerison and Corsellis, 1966; Babb *et al.*, 1984), network reorganization (Sutula *et al.*, 1989; Parent and Lowenstein, 1997), as well as alterations of receptor

and ion channel functions (Steinhäuser and Seifert, 2002; Avanzini and Franceschetti, 2003). In addition, functional neuroimaging studies demonstrated a decrease in glucose utilization ('hypometabolism') in seizure foci and adjacent brain structures of epilepsy patients (Kuhl *et al.*, 1980; O'Brien *et al.*, 1997; Casse *et al.*, 2002), which might be explained by dysfunction of mitochondrial oxidative and/or glycolytic energy metabolism. However, no record exists of detailed investigation of metabolic and mitochondrial functions during neuronal activation in the *ex vivo* hippocampus from TLE patients.

In the brain, the functional integrity of mitochondria is essential because these organelles generate most of the ATP that is used for ion transport, maintenance of excitability and neurotransmission (Ames, 2000). In mitochondria, reduced nucleotides, NADH and $FADH_2$, mainly serve in energy transfer and connect dehydrogenase activity within the Krebs–Szentgyörgyi cycle to oxidative phosphorylation (McCormack *et al.*, 1990; Hansford and Zorov, 1998). Monitoring NAD(P)H fluorescence provides insight into the status of both oxidative and glycolytic energy metabolism, e.g. in brain slice preparations (Lipton, 1973; Schuchmann *et al.*, 2001; Kann *et al.*, 2003*a*, *b*; Shuttleworth *et al.*, 2003).

Neuronal activation results in the release of potassium to extracellular space (Heinemann *et al.*, 1990). Electrophysiological recordings of the extracellular potassium concentration ($[K^+]_o$) indicate the degree of local activity from neurons neighbouring the recording site (Heinemann and Lux, 1975). Thus, simultaneous recordings of $[K^+]_o$ and NAD(P)H fluorescence have been used to examine the coupling of neuronal activity and energy metabolism (Lewis and Schuette, 1975; Kann *et al.*, 2003*a*, *b*).

The present study was designed to explore cellular metabolic and mitochondrial functions in the *ex vivo* hippocampus from pharmaco-resistant TLE patients during neuronal activation that was elicited by electrical stimulation or glutamate application. To be able to determine alterations of stimulus-induced NAD(P)H fluorescence transients, we controlled the induction of neuronal activation in tissue with varying degrees of neuronal cell loss by simultaneous monitoring of $[K^+]_o$. Using the cationic dye, Rhodamine-123 we examined the inner membrane potential of mitochondria ($\Delta\Psi_m$) in slices and individual neurons. Because of the lack of human control tissue, we related our findings from TLE patients to tissue from chronic epileptic rats utilizing the 'pilocarpine model' of experimental TLE (Cavalheiro *et al.*, 1991; Mello *et al.*, 1993).

Methods

Pilocarpine-treated rats and TLE patients

Status epilepticus was induced in male Wistar rats (115–130 g) by injection of pilocarpine hydrochloride (320 mg/kg, i.p.; Sigma-Aldrich, Taufkirchen, Germany) 30 min after pre-treatment with scopolamine hydrobromide (1 mg/kg, s.c.; Sigma-Aldrich) to reduce peripheral cholinergic effects. After 1.5 h, status epilepticus was terminated by diazepam injection (5–10 mg/kg, i.p.; Ratiopharm, Ulm, Germany). After 90 and 210 min, Ringer solution supplemented with lactate (27.2 mM; Sigma-Aldrich) and sodium hydrogen carbonate (71 mM; Sigma-Aldrich) was injected (i.p.) to improve survival. Control rats were treated with the same protocol, but with saline instead of pilocarpine. Rats were kept in separate cages under standard housing conditions. All rats were monitored by video recordings to assure development of spontaneous epileptic activity: a seizure-free interval of two to three weeks was followed by spontaneous recurrent seizures that lasted as long as the animals were alive (Mello *et al.*, 1993; Lehmann *et al.*, 2001). Recurrent seizures were characterized by oral automatism, head and bilateral forelimb myoclonus, rearing, falling and loss of consciousness. Seizure frequency of pilocarpine-treated rats was 0.7 ± 0.4 ($n = 8$) per day. Rats ($n = 15$) were killed 7.7 ± 0.9 months after pilocarpine-induced status epilepticus (and sham treatment). Animal experiments were conducted in accordance with the guidelines of the European Communities Council and approved by the Regional Berlin Animal Ethics Committee (G0328/98, G0024/04).

All the 16 patients with pharmaco-resistant TLE involved in this study had undergone partial unilateral resection of the hippocampus (performed by T.-N. Lehmann), i.e. of the anterior half of the hippocampal body ~20 mm posterior from the tip of the inferior horn of the lateral ventricle. The diagnosis was made in the Epilepsy Center of Berlin-Brandenburg (Herzberge) according to European Guidelines for pre-surgical evaluation (European Federation of Neurological Societies Task Force, 2000). The study was approved by the Ethics Committee at Charité (EA125/2001, EA1/042/04) and in accordance with the 'Declaration of Helsinki'. Each patient gave an informed consent in written form for studies on resected tissue.

After histopathological diagnosis (Institute for Neuropathology, Charité), tissue from TLE patients was assigned to a group characterized by AHS (Wyler grades III and IV) and a group without AHS (non-AHS group; Wyler grades I and II) (Wyler *et al.*, 1992).

Tissue preparation

Resected human hippocampal tissue was immediately immersed in oxygenated solution (95% O_2, 5% CO_2, 4°C) and cut in tissue blocks of 2–4 mm to facilitate oxygen penetration during transport (30 min). The solution contained in mM: KCl 3, NaH_2PO_4 1.25, glucose 10, $MgSO_4$ 2, $MgCl_2$ 2, $CaCl_2$ 1.6, $NaHCO_3$ 21, sucrose 200 and α-tocopherol 0.1 (pH 7.4). Sodium was reduced to prevent hypoxia-induced Na^+-influx to neurons while α-tocopherol was added for scavenging free radicals. After transport, tissue blocks were immediately cut into slices. Using this approach, we were able to record neuronal responses and evoked epileptiform activity in resected tissue from >60 TLE patients over hours after surgery (Kivi *et al.*, 2000; Gabriel *et al.*, 2004). Rats were decapitated under deep diethylether anaesthesia and their brains were quickly removed. Horizontal and coronal hippocampal slices (450 μm) were prepared from rat and human material, respectively, in ice-cold, oxygenated (95% O_2, 5% CO_2) artificial cerebrospinal fluid (ACSF), using a vibratome (Campden, Leicester, UK) and directly transferred to an incubation chamber. Slices were incubated in ACSF for 2–4 h to recover from the preparation procedure (room temperature) before being used for experiments (superfusion with ACSF, 4 ml/min, 33–35°C). ACSF contained (in mM): NaCl 129, KCl 3, NaH_2PO_4

1.25, $MgSO_4$ 1.8, $CaCl_2$ 1.6, $NaHCO_3$ 21 and glucose 10 (pH 7.4). All salts and α-tocopherol were from Sigma-Aldrich.

Measurements of $[K^+]_o$ and microfluorimetry of NAD(P)H and rhodamine-123

DC-coupled recordings of field potentials and changes in $[K^+]_o$ were performed with double-barrelled K^+-sensitive and reference microelectrodes (Heinemann and Arens, 1992). In brief, electrodes were pulled from double-barrelled theta glass (Science Products, Hofheim, Germany). The reference barrel was filled with 154 mM NaCl solution, the ion-sensitive barrel with potassium ionophore I cocktail A (60031; Fluka Chemie, Buchs, Switzerland) and 100 mM KCl. Electrodes with a sensitivity of 59 ± 2 mV to a 10-fold increase in $[K^+]$ were used for experiments. The amplifier was equipped with negative capacitance feedback control, which permitted recordings of changes in $[K^+]_o$ with time constants of 50–200 ms.

The recording electrode was positioned in the neuronal cell somata layer and in the centre of the fluorescence recording area (×20 objective, 0.5 numerical aperture; Zeiss, Jena, Germany). The neuronal compartment was activated by electrical stimulation (20 Hz, 10 s, 1–10 V) of stratum radiatum for recordings in CA3, CA1 and the subiculum as well as of the perforant path for recordings in the dentate gyrus (DG). The bipolar stimulation electrode was positioned 600–700 μm apart from the recording electrode to avoid direct depolarization of the astrocytic compartment within the recording area. NAD(P)H was excited at 360 nm (monochromator; Photon Technology Instruments, Wedel, Germany) and fluorescence emission was recorded at 460 nm using a photomultiplier (Seefelder Messtechnik, Seefeld, Germany) mounted on an epifluorescence microscope (Axioskop, Zeiss). In contrast to oxidized forms, reduced nicotinamide dinucleotides, NADH and NADPH, fluoresce when excited by ultraviolet light (Aubin, 1979). In mitochondria, NAD^+ is reduced to NADH by several dehydrogenases, and $NADP^+$ is reduced to NADPH by isocitrate dehydrogenase as well as by transhydrogenase activity at the expense of NADH (Jackson, 2003). In the cytosol, NAD^+ is reduced within the second part of the glycolysis. Because the emission spectra of NADH and NADPH overlap, NAD(P)H indicates that recorded fluorescence might have originated from either one or both (Schuchmann *et al.*, 2001). For microfluorimetric rhodamine-123 recordings in AHS tissue, slices from patients with numbers 14, 15 and 16 were bulk-loaded with rhodamine-123 for 10 min (Sigma-Aldrich; stock solution in ethanol, 5 μM final concentration) and incubated for another 60 min in ACSF at room temperature. Rhodamine-123 was excited at 490 nm and fluorescence emission was recorded at 515–530 nm.

Fluorescence data and changes in voltage of the recording electrode were digitized at 10 Hz using a standard PC and FeliX software (Photon Technology Instruments). Changes in NAD(P)H and rhodamine-123 fluorescence are presented as $\Delta F/F_0$ in %. Rhodamine-123 fluorescence baseline shift was corrected offline. Changes in $[K^+]_o$ are presented in mM. To translate the recorded potential values (mV) in $[K^+]_o$, a modified Nernst equation was used:

$$\log[\mathrm{Ion}]_1 = E_M * (s * v)^{-1} + \log[\mathrm{Ion}]_o,$$

with E_M, recorded potential; s, electrode slope obtained at calibration; v, valence of the specific ion; $[\mathrm{Ion}]_o$, ion concentration at rest; and $[\mathrm{Ion}]_1$, ion concentration during activation.

Intracellular recordings and rhodamine-123 imaging

Slices from patients with numbers 3, 4, 5, 6 and 7 were fixed with a platinum wire in the recording chamber mounted on an epifluorescence microscope (BX50WI, Olympus, Hamburg, Germany) and superfused with ACSF at 4 ml/min. Patch pipettes (4–5 MΩ resistance) were pulled with a horizontal puller (Sutter Instruments Corp., Novato, CA, USA). The pipette solution contained (in mM): KGlu 135, NaCl 10, $CaCl_2$ 0.05, EGTA 1, HEPES 10, MgATP 3 (Sigma-Aldrich) at pH 7.3 (275–290 mOsmol/kg). Current-clamp recordings of neurons were performed in the whole-cell configuration using a patch-clamp amplifier, EPC 7 (Heka Elektronik GmbH, Lambrecht/Pfalz, Germany), IBM-compatible PC and WinTida 4.0 (Heka). Series resistance and input resistance were 12 ± 1.2 MΩ and 48 ± 3.8 MΩ (mean ± SE; $n = 8$), respectively.

Recordings of changes in $\Delta\Psi_m$ were performed as described (Schuchmann *et al.*, 2000). In brief, membrane-permeable, cationic fluorescent dye, rhodamine-123 (10 μg/ml, stock solution in ethanol) was added to the pipette solution. The dye was allowed to diffuse to the cytoplasm for 20–30 min, after establishing the whole-cell patch. Due to its cationic nature, rhodamine-123 accumulates in respiring mitochondria that maintain a negative $\Delta\Psi_m$. In mitochondria, fluorescence intensity of rhodamine-123 is quenched due to matrix protein binding. Upon mitochondrial depolarization, the dye is released to the cytoplasm and de-quenched resulting in a cytoplasmic increase in rhodamine-123 fluorescence intensity (Bindokas *et al.*, 1998; Ward *et al.*, 2000). Fluorescence recordings were performed using a NORAN Oz confocal laser scanning microscope (Prairie Technologies Inc., Middleton, WI, USA) with acquisition software (Intervision, Irix 6.3, Silicon Graphics, Mountain View, CA, USA). Rhodamine-123 was excited using the 488 nm line of a krypton–argon laser (Omnichrom 643, Melles Griot, Bensheim, Germany) with an intensity of <10 μW as determined under the objective. Fluorescence was measured with a water immersion objective (×60, 0.9 numerical aperture, Olympus, Hamburg, Germany). The pinhole was set to 50–100 μm and averaged (8–16 frames) 8-bit images were captured at 1–2 Hz. The focal plane contained the soma and primary dendrites of a neuron. Changes in rhodamine-123 fluorescence were evaluated offline using the ImageJ (RSB, NIMH, Bethesda, MD, USA). Changes in fluorescence were determined in the cytoplasm by setting regions of interest and are expressed as $\Delta F/F_0$ in % after baseline correction (Kovács *et al.*, 2005).

Cresyl violet staining

Slices from rats and humans were fixed in paraformaldehyde (4%, 0.1 M phosphate buffer; Sigma-Aldrich), after the preparation procedure. For further processing, fixed slices were incubated with sucrose solution (30%, 0.15 M phosphate buffer; Sigma-Aldrich) for 12–16 h, and 30 μm sections were prepared using a freezing microtom (Leica Microsystems, Wetzlar, Germany). Sections were exposed to an ethanol series (6 steps, 3 min each) and rinsed in distilled water. Sections were then immersed in cresyl violet solution (0.5% cresyl violet in distilled water; Sigma-Aldrich) for 90 s, rinsed in distilled water, and transferred to differentiation solution (200 ml, 50% ethanol, 3 drops of acetic acid). Subsequently, sections were exposed to a series of ethanol (4 steps, 3 min each), 2-propanol (two times; Sigma-Aldrich), and xylol (two times; Sigma-Aldrich) and finally embedded with DePeX (Serva Electrophoresis GmbH, Heidelberg,

Germany). Sections were analysed using an upright Axioskop (Zeiss) equipped with a CCD camera (DX30; Kappa optoelectronics, Gleichen, Germany). Images were processed with ImageBase Control® (Kappa).

Statistics

Experimental data (*n*) from different areas of the hippocampus were obtained from slices of 8 pilocarpine-treated rats, 7 control rats, 11 AHS and 5 non-AHS patients. Results of a particular experiment were pooled and are given as mean ± SE. For a given parameter (e.g. overshoot in NAD(P)H transient), two groups, either of the rat preparation (control versus pilocarpine-treated rats) or of the human preparation (non-AHS versus AHS), were compared in a given region (e.g. area CA1) using one way ANOVA.

Results

Histopathology of chronic epileptic tissue

Eight pilocarpine-treated rats that had developed spontaneous recurrent seizures (grade 5 on the Racine scale) (Racine, 1972) were included in the present study. In these animals, neuronal cell loss occurs predominantly in the medial entorhinal cortex and in the hippocampal formation (Du *et al.*, 1995). Within the hippocampal formation, the hilus, area CA3 and area CA1 are significantly more affected than the subiculum (Mello *et al.*, 1993; Fig. 1A–D). These findings correspond well to histopathological alterations of AHS tissue from TLE patients (Babb *et al.*, 1984; Blümcke *et al.*, 1999) making pilocarpine-treated rats a useful and reliable model for TLE (Cavalheiro *et al.*, 1991; Mello *et al.*, 1993).

Histopathology of tissue from pharmaco-resistant TLE patients revealed AHS (Wyler grades III and IV) in 11 and less neuronal cell loss (non-AHS; Wyler grades I and II) in 5 of the resected hippocampi (Fig. 1E–H). The age of the patients ranged from 19 to 56 years. Mean age and mean duration of TLE within the AHS group (non-AHS group) were 33.6 ± 4.0 (29.6 ± 3.9; $P = 0.5$) and 26.1 ± 3.6 (13.9 ± 5.2; $P = 0.08$) years, respectively. Table 1 contains the details on patient data.

Alterations of NAD(P)H transients in chronic epileptic tissue

We recorded NAD(P)H fluorescence to investigate cellular energy metabolism during neuronal activation in different areas of acute hippocampal slices from rats and humans. Neuronal activation was elicited by electrical stimulation (10 s, 20 Hz) and resulted in transient increases in $[K^+]_o$ of up to 2.3 mM (Fig. 2), corresponding to the upper range of *in vivo* responses to sensory and electrical stimuli (Heinemann *et al.*, 1990; Somjen, 1995).

As expected, stimulus-induced neuronal activation was closely associated with characteristic biphasic NAD(P)H fluorescence transients in control rats. The transients consisted of a brief initial 'drop' that was followed by a prolonged 'overshoot' of up to several minutes (Fig. 2A). Such biphasic NAD(P)H transients have been described in a variety of neuronal preparations (Lipton, 1973; Duchen, 1992; Schuchmann *et al.*, 1998; Kann *et al.*, 2003*a, b*). In contrast, stimulus-induced NAD(P)H transients were altered in chronic epileptic tissue. The overshoot was smaller in area CA1 from chronic epileptic rats (Fig. 2B) and absent in many experiments in tissue from TLE patients, although increases in $[K^+]_o$ reflected substantial neuronal activation (Fig. 2C, D and F).

In Fig. 3, we summarize the quantification of drops and overshoots as well as of increases in $[K^+]_o$ in area CA1 and the subiculum of the rat preparation (control versus pilocarpine-treated group) and the human preparation (non-AHS versus AHS group). To be able to compare the groups, we included all recordings with increases in $[K^+]_o$ of <1.6 mM. Notably, the overshoots were significantly smaller in area CA1 of the pilocarpine-treated group, while the drops were similar as compared to the control (Fig. 3A). Similar increases in $[K^+]_o$ in both groups broadly excluded the possibility that the difference in overshoots was because of lower neuronal activation in pilocarpine-treated rats, e.g. because of sclerosis. In the subiculum, we found no significant differences between both groups, indicating a region-specific alteration of NAD(P)H transients in chronic epileptic rats. In tissue from TLE patients, the findings were more complex. In a few experiments, neuronal activation was associated with overshoots of up to 2.3% (Fig. 2C and D, plots). Largest overshoots were observed in patients with numbers 1, 6 and 10. Interestingly, they only differed from the other patients ($n = 13$) in age of TLE onset (26.3 ± 3.5 versus 6.4 ± 1.7 years; $P = 0$) and seizure frequency (13.3 ± 4.9 versus 6.2 ± 1.1 per month; $P = 0.04$). We rate this to be a trend because of the small number of *n*. In the majority of experiments, we observed very small overshoots in both area CA1 and the subiculum that went along with large drops (Fig. 3B). Moreover, these alterations of NAD(P)H transients were independent of the degree of sclerosis, because there were no significant differences when comparing AHS and non-AHS groups in both areas. Alterations were also found in area CA3 ($n = 6$, 3 patients) (not shown) and the DG of human tissue (Fig. 2F).

Stimulus-induced NAD(P)H transients indicate adaptation of mitochondrial oxidative and glycolytic metabolism (Lipton, 1973; Schuchmann *et al.*, 2001), and the alterations suggest severe metabolic dysfunction in chronic epileptic tissue. Because mitochondria are the major source of energy supply in the CNS (Ames, 2000), alterations of NAD(P)H transients may reflect chronic defects of mitochondrial enzymes and/or membrane properties.

Negative mitochondrial membrane potential in chronic epileptic tissue

Respiring mitochondria establish a negative $\Delta\Psi_m$ that is essential for substrate cycling, Ca^{2+}-uptake via the uniporter, and ATP synthesis (McCormack *et al.* 1990; Hansford and Zorov, 1998; Nicholls and Budd, 2000), and the significant

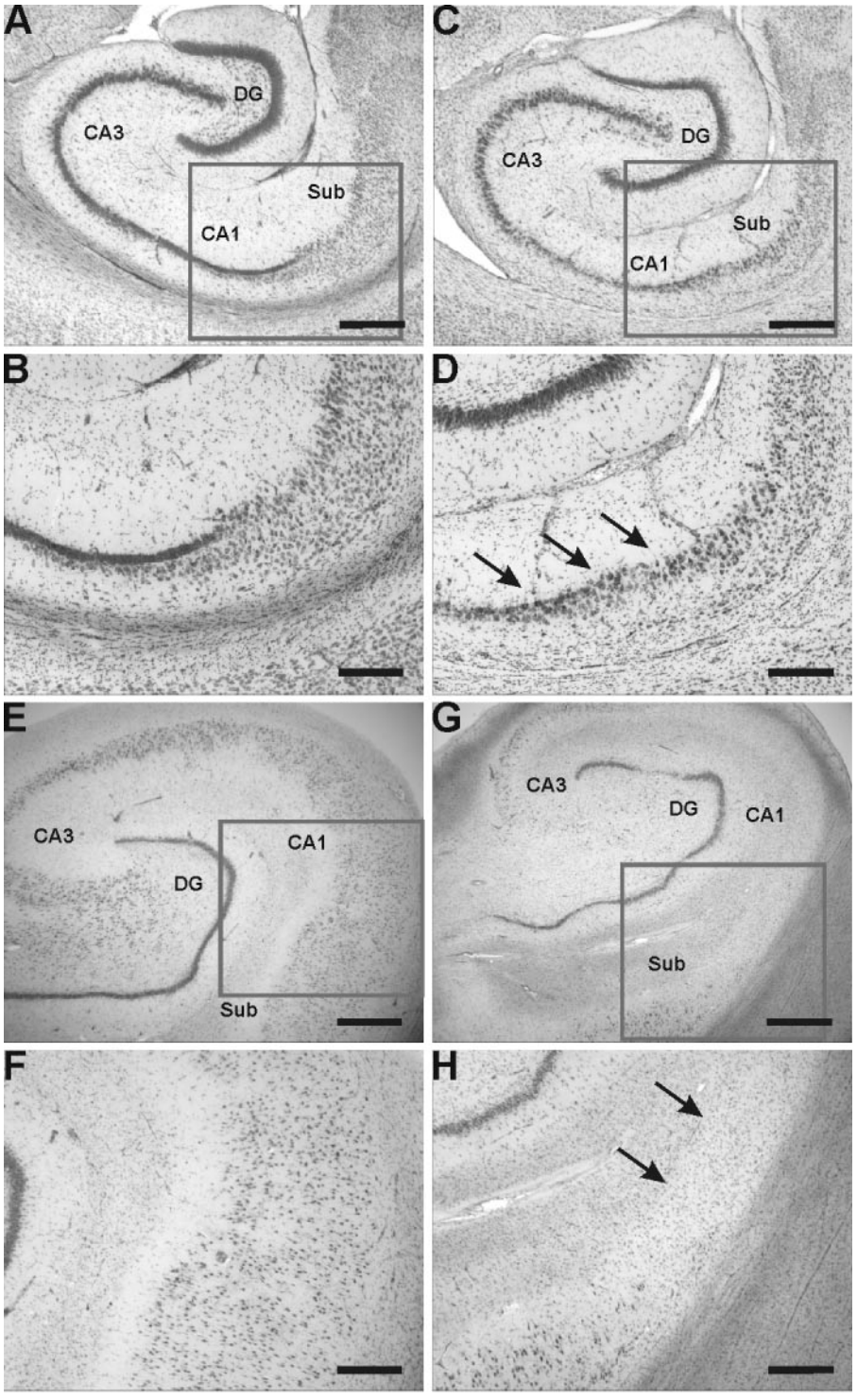

Fig. 1 Histopathology of chronic epileptic tissue. Neurons in acute hippocampal slices were stained with cresyl violet to uncover cell loss and dispersion of cell layers in tissue from chronic epileptic rats and temporal lobe epilepsy patients. (**A**) Hippocampal slices of control rats are characterized by dense formation of neuronal cell somata in areas CA3, CA2 and CA1, as well as of granule cells in the DG (scale bar denotes 500 μm). (**B**) Magnification of the transition from area CA1 to the subiculum (Sub) [rectangular marked region in (A)] reveals typical dispersion of cell somata layer in subiculum without cell loss (scale bar denotes 250 μm). (**C**) and (**D**) Hippocampal slices of pilocarpine-treated rats are characterized by pronounced neuronal cell loss and dispersion of the cell somata layer in area CA1 (black arrows; scale bars in C and D denote 500 and 250 μm, respectively). (**E**) Hippocampal slice from a TLE patient without AHS (non-AHS, scale bar denotes 1 mm). (**F**) Magnification of transition from area CA1 to subiculum [rectangular marked region in (**E**)] reveals dispersion of the cell somata layer with a still considerable density of neurons (scale bar denotes 500 μm). (**G**) and (**H**) Hippocampal slice of a TLE patient with AHS is characterized by pronounced neuronal cell loss in area CA1 and proximal subiculum (black arrows; scale bars in G and H denote 1 mm and 500 μm, respectively).

Table 1 Patient data

	Gender	Age	Duration	Location	Histopathology	Rates
1	F	34	2	Left	I	5/0
2	F	48	40	Left	III	8/0.2
3	M	20	11	Left	III	12/4
4	F	37	17	Left	III	3/0
5	F	20	19	Right	III	3/1.5
6	M	49	22	Right	III	22/0.1
7	F	21	18	Right	IV	7/0.1
8	F	21	20	Left	I	14/0
9	M	36	28	Right	I	7/0
10	F	38	18	Left	I	13/4
11	F	40	36	Left	III	2/2
12	F	21	20	Left	III	2/0
13	M	19	1.5	Left	II	6/2
14	F	33	30	Left	III	10/0
15	M	56	52	Right	III	3/0.1
16	F	25	22	Right	IV	4/0

The table includes gender, age at surgery, duration of TLE (given in years), location of the resected hippocampus, histopathology (determined by Wyler grading), and seizure rate/secondary generalized seizure rate (given per month/year).

role of mitochondrial Ca^{2+}-uptake in regulation of $NAD(P)^+$ reduction has been reported in a variety of cell types (Robb-Gaspers *et al.*, 1998; Kann *et al.*, 2003*a*, *b*; Bruce *et al.*, 2004). Therefore, monitoring the changes of $\Delta\Psi_m$ during neuronal activation with mitochondria-specific, voltage-sensitive dye (rhodamine-123) provided an opportunity to prove whether (chronically) collapsed $\Delta\Psi_m$ of mitochondria was one of the mechanisms underlying alterations of NAD(P)H transients. To sufficiently activate all neurons, we applied glutamate via the bath solution.

Glutamate elicited similar $\Delta\Psi_m$ responses in area CA1 of both chronic-epileptic and control rats ($n = 8$, two animals, each) that were bulk-loaded with rhodamine-123 (Fig. 4A). Subsequent application of mitochondrial uncoupler, carbonyl cyanide *m*-chlorophenyl hydrazone (CCCP) (Nicholls and Budd, 2000; Kann *et al.*, 2003*a*), revealed the overall capacity of mitochondria to accumulate rhodamine-123 owing to negative $\Delta\Psi_m$. The same experiment was performed in area CA1 of three AHS patients revealing $\Delta\Psi_m$ responses in the similar range (Fig. 4A). To control the degree of neuronal activation as elicited by glutamate, we tested its effects on NAD(P)H fluorescence and $[K^+]_o$ in area CA1 of AHS tissue (Fig. 4B). As with electrical stimulation, glutamate application resulted in a transient increase in $[K^+]_o$ (1.1 ± 0.5 mM, $n = 3$, three AHS patients) while the overshoot of NAD(P)H transients remained small ($1.4 \pm 0.3\%$). The different time course of changes in NAD(P)H and $[K^+]_o$ was probably due to the prolonged duration of glutamate application (60 s). Nevertheless, regarding the increase in maxima of the transients, this experiment confirmed that both stimulation protocols elicited neuronal activation in a similar range.

To verify mitochondrial responses in individual neurons of human tissue, we combined patch-clamp recordings and confocal laser scanning microscopy. Visually identified neurons ($n = 8$, five AHS patients) were investigated in area CA1 and the proximal subiculum in AHS tissue, where alterations of NAD(P)H transients were most prominent. Twenty to thirty minutes after establishing a whole-cell patch with pipette solution that contained rhodamine-123, a bright dotted staining pattern of mitochondrial structures developed while cytoplasmic rhodamine-123 fluorescence remained weak. Confocal imaging allowed for depiction of individual mitochondria in the somata of the neurons (Fig. 5A and B), which was a first indication of mitochondria that maintained a negative $\Delta\Psi_m$. All investigated neurons ($n = 8$) responded to glutamate with a depolarization of 48.1 ± 6 mV from a resting cell membrane potential of -57.4 ± 2 mV (Fig. 5C). Application of glutamate was repeated in four of these neurons after the cell membrane potential had recovered to baseline (308 ± 62 s), which resulted in similar depolarization (not shown). In all neurons ($n = 8$), cytoplasmic rhodamine-123 fluorescence intensity increased after a glutamate-induced train of action potentials (Fig. 5C). Fluorescence intensity reached maximum of $103.8 \pm 29\%$ almost simultaneously with the peak of cell membrane depolarization (after 131 ± 35.8 s) and recovered slowly. This range of fluorescence intensity corresponded to that obtained in activated neurons in a non-epileptic rat slice preparation applying the same recording and evaluation methods (Kovács *et al.*, 2005), which strongly supports our data from bulk-loaded slices (Fig. 4A). Note that confocal imaging from regions of interest in individual neurons provides fluorescence signals in a higher order of magnitude as compared to the totalized microfluorimetric signal from neurons and glial cells of bulk-loaded slices (Kovács *et al.*, 2002).

These data showed that mitochondria in chronic epileptic tissue, even in individual neurons, maintained a negative $\Delta\Psi_m$ and depolarized during neuronal activation; although $NAD(P)^+$ reduction was significantly impaired in the respective hippocampal regions. This might indicate defects on the mitochondrial enzyme level rather than on mitochondrial membrane properties.

Discussion

The main findings of the present study are significant alterations of NAD(P)H fluorescence transients during neuronal activation in acute hippocampal slices from chronic epileptic rats and humans, although mitochondria maintain negative $\Delta\Psi_m$. These findings provide a cellular correlate for 'hypometabolism' as described for epilepsy patients and, thereby, suggest mitochondrial enzyme defects in TLE.

Induction of similar neuronal activation

K^+-sensitive microelectrodes measure accumulation of potassium in a restricted extracellular space (Heinemann and Lux, 1975). The electrodes detect changes in $[K^+]_o$ in a distance of at least 150 μm, and were positioned in the centre

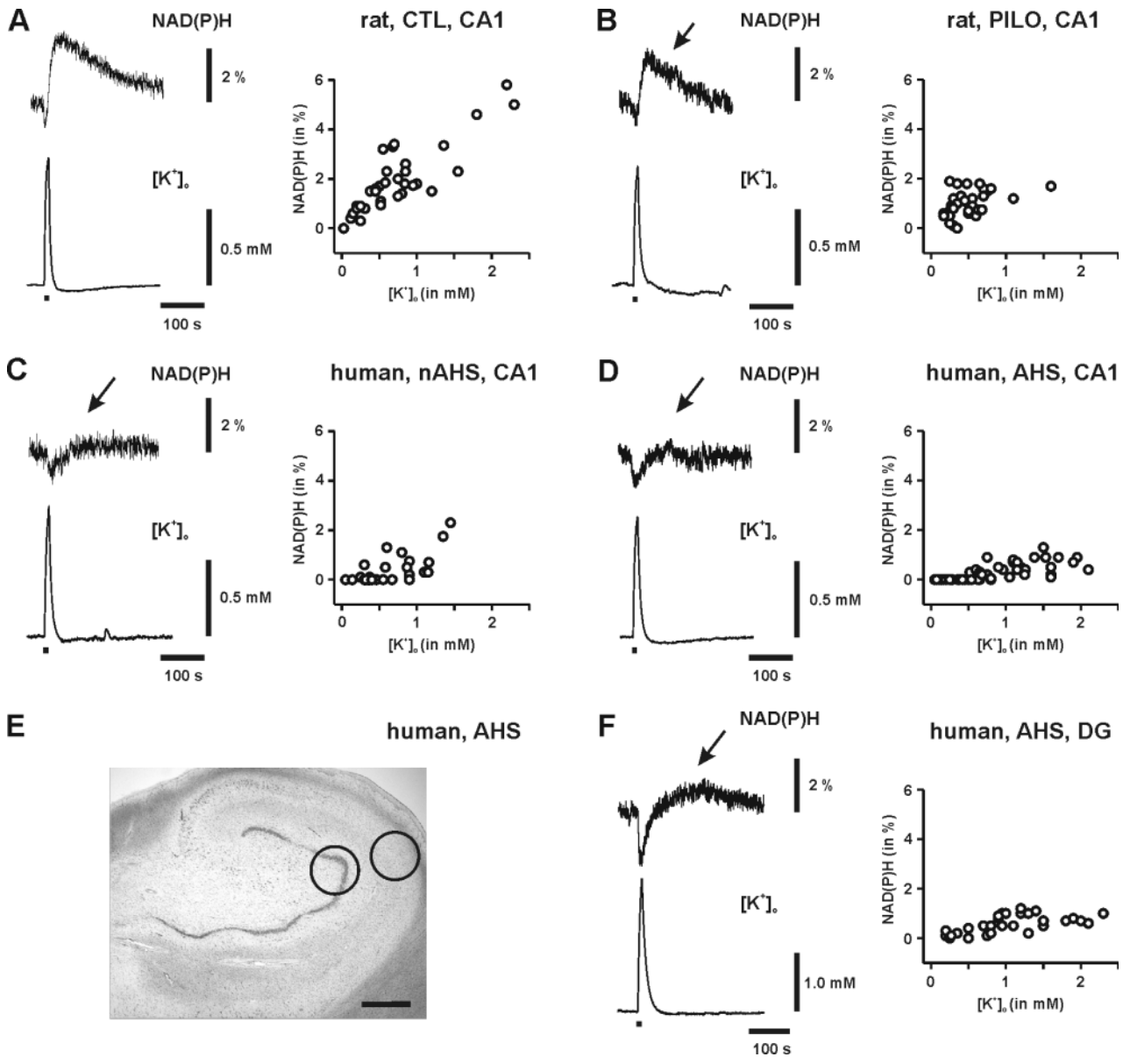

Fig. 2 Stimulus-induced transients of NAD(P)H fluorescence and $[K^+]_o$. The traces illustrate simultaneous recordings of NAD(P)H fluorescence and $[K^+]_o$ in area CA1 of acute hippocampal slices from five control (CTL) and six pilocarpine-treated (PILO) rats (**A** and **B**, left), from five TLE patients without (nAHS) and eleven with AHS (**C** and **D**, left) as well as from the DG from TLE patients with AHS (**F**, left). NAD(P)H fluorescence was recorded in circumscribed regions of hippocampal slice preparations while changes in $[K^+]_o$ were measured in their centres by using ion-sensitive electrodes (**E**). The scheme shows fluorescence recordings in the DG (left circle) and in area CA1 (right circle). (**A**) Neuronal activation, as elicited by application of electrical stimulation (10 s, 20 Hz, black bar), was tightly associated with characteristic biphasic NAD(P)H fluorescence transients. NAD(P)H transients consisted of a brief initial 'drop' and a subsequent prolonged 'overshoot' of up to several minutes (upper trace). (**B**) In pilocarpine-treated rats, the overshoot of NAD(P)H transients was smaller (upper trace, arrow). (**C**, **D** and **F**) In the majority of experiments in tissue from TLE patients overshoots were very small (upper traces, arrows) though transient increases in $[K^+]_o$ (lower traces) reflected substantial neuronal activation. Note that $[K^+]_o$ was simultaneously monitored to judge the degree of neuronal activation in the acute slices. Electrical stimulation resulted in a transient increase in $[K^+]_o$ that was followed by a slight baseline undershoot with recovery over minutes (lower traces; Heinemann and Lux, 1975, Kann *et al.*, 2003*a*). The plots represent the overshoots of stimulus-induced NAD(P)H transients as a function of transient increases in $[K^+]_o$ from $n = 33$ (**A**), $n = 35$ (**B**), $n = 25$ (**C**), $n = 49$ (**D**) and $n = 29$ (**F**).

of a region of interest. We assume that, thereby, monitoring of $[K^+]_o$ widely reflected the degree of neuronal activation in the region where NAD(P)H fluorescence was recorded. For quantitative comparison of NAD(P)H transients, this enabled us to elicit similar neuronal activation in hippocampal slices with different degrees of sclerosis. However, since there is some evidence for an impairment of glial K^+-uptake mechanisms in area CA1 of AHS tissue (Kivi *et al.*, 2000; Hinterkeuser *et al.*, 2000), neuronal activation might have been overestimated in this region. This might partially

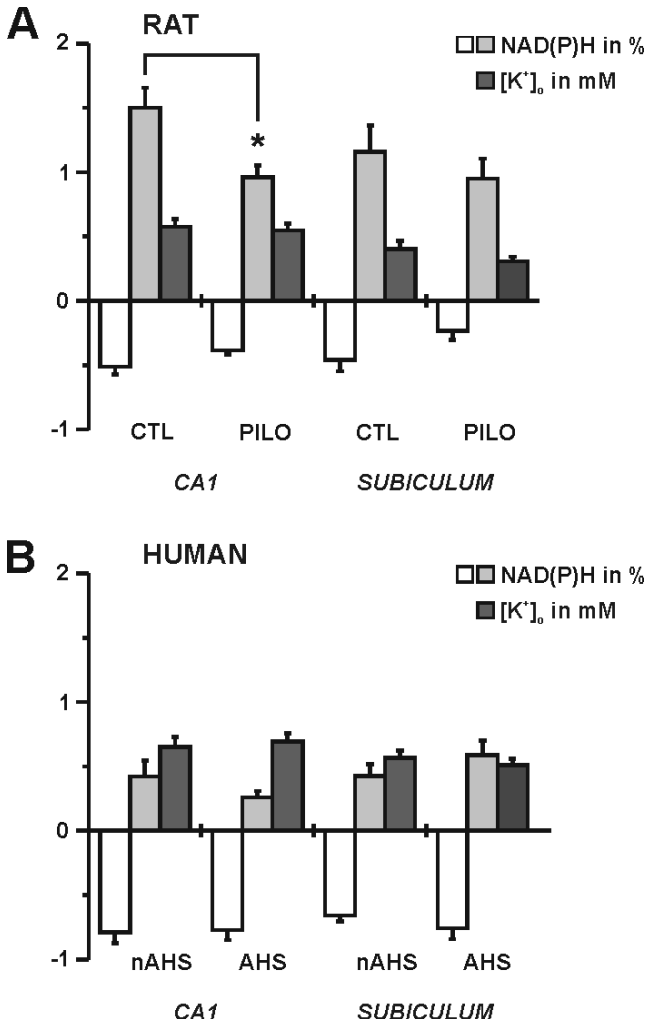

Fig. 3 Bar graph on components of stimulus-induced NAD(P)H fluorescence transients. The bar graphs illustrate a quantification of components of NAD(P)H transients from measurements in control (CTL) and pilocarpine-treated, chronic epileptic rats (PILO) (**A**) as well as in non-AHS (nAHS) and AHS tissue from TLE patients (**B**). For each measurement, we determined the drop (white columns) and the overshoot (light grey columns) of stimulus-induced NAD(P)H transients, as well as the increase in $[K^+]_o$ (dark grey columns) that were simultaneously recorded. The bar graphs summarize data from the rat preparation in area CA1 (CTL, $n = 30$; PILO, $n = 34$) and subiculum (CTL, $n = 14$; PILO, $n = 12$), as well as the human preparation (CA1; nAHS, $n = 25$; AHS, $n = 43$) (subiculum; nAHS, $n = 26$; AHS, $n = 28$). (**A**) In area CA1 of pilocarpine-treated rats, the overshoots were significantly smaller ($P < 0.001$), while the difference in drops was not significant ($P = 0.06$) as compared to the control. In the subiculum, the differences in drops and overshoots were not significant ($P = 0.06$ and $P = 0.44$). Note that similar increases in $[K^+]_o$ in control and pilocarpine-treated rats indicate virtually the same degree of neuronal activation (CA1, $P = 0.74$; subiculum, $P = 0.23$). (**B**) In area CA1 and the subiculum of AHS tissue, the differences in both drops and overshoots were not significant as compared to non-AHS tissue (CA1: $P = 0.87$ and $P = 0.15$; subiculum: $P = 0.32$ and $P = 0.26$). Note that large drops went along with very small overshoots in both area CA1 and the subiculum. Increases in $[K^+]_o$ in AHS and non-AHS tissue were not significantly different (CA1, $P = 0.71$; subiculum, $P = 0.46$).

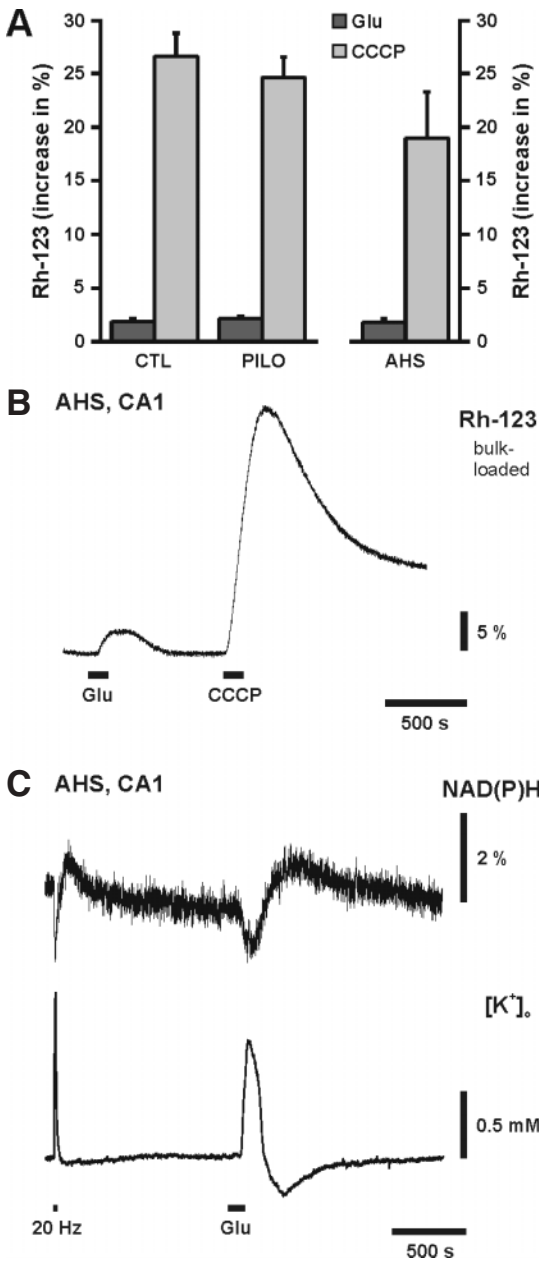

Fig. 4 Changes in rhodamine-123 fluorescence, NAD(P)H fluorescence and $[K^+]_o$ in area CA1 from rats and humans. (**A**) The bar graphs illustrate the quantification of $\Delta\Psi_m$ responses as elicited by glutamate (Glu, dark grey columns) and mitochondrial uncoupler (CCCP, light grey columns) in area CA1 of slices from control (CTL, $n = 8$) and chronic-epileptic rats (PILO, $n = 8$; $P = 0.48$ and $P = 0.51$, respectively), which were bulk-loaded with rhodamine-123. Area CA1 of slices from AHS patients showed $\Delta\Psi_m$ responses in the similar range (AHS, $n = 4$). (**B**)The example trace from area CA1 of slices from AHS tissue illustrates bath application of glutamate (Glu, 300 μM) and CCCP (1 μM) (black bars). (**C**) Electrical stimulation (20 Hz, 10 s, black spot) and glutamate application (Glu, 300 μM, black bar) were performed in area CA1 of AHS tissue while simultaneously monitoring NAD(P)H fluorescence (upper trace) and $[K^+]_o$ (lower trace). Note that, transient increases in $[K^+]_o$ indicate neuronal activation in a similar range as induced by both electrical stimulation and glutamate application.

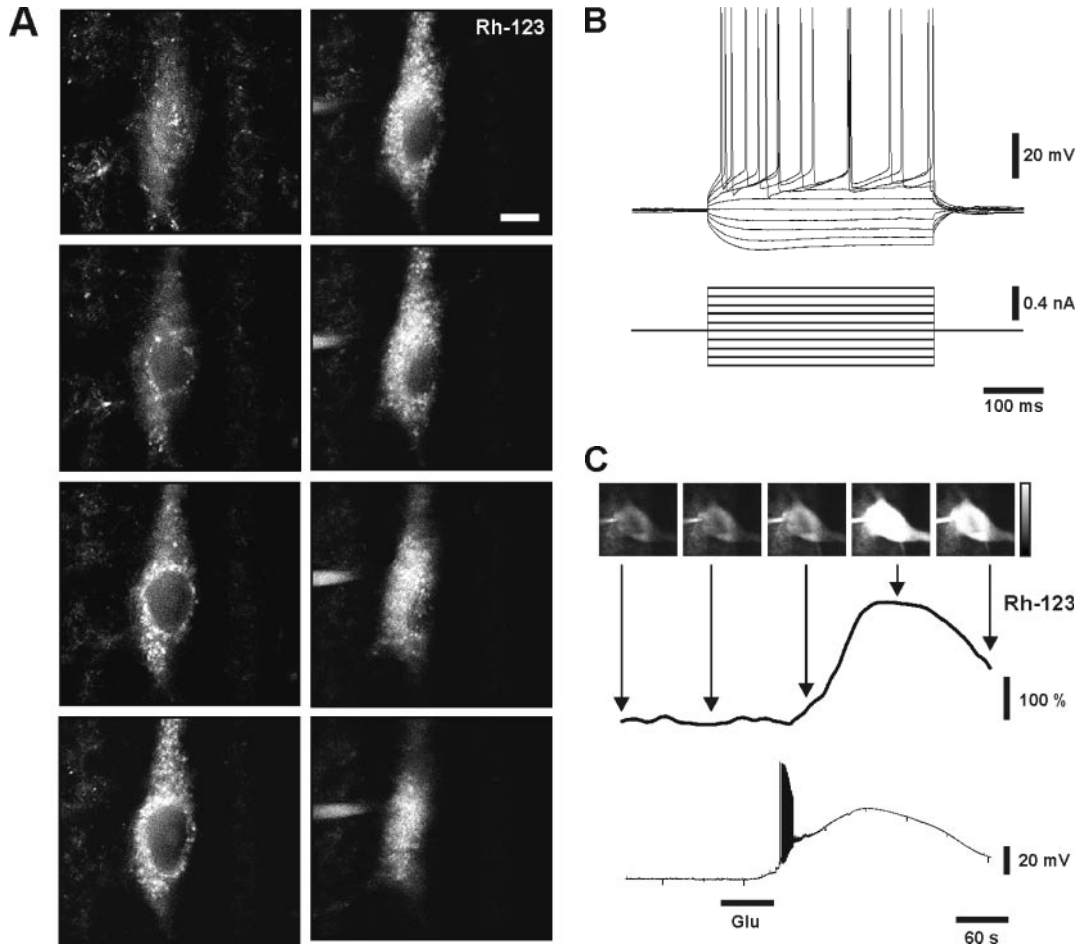

Fig. 5 Changes in rhodamine-123 fluorescence and cell membrane potential in individual neurons of human tissue. (**A**) In area CA1 and the proximal subiculum of AHS tissue, neurons were visually identified and patched using a pipette solution that contained cationic dye, rhodamine-123 (Rh-123). Confocal *xy*-*z* scan (step size 2 μm; scale bar 10 μm) allowed us to illustrate the distribution of mitochondria in patched neurons. Most of the mitochondria were located in the perinuclear region. Note that accumulation of rhodamine-123 indicates negative $\Delta\Psi_m$ of mitochondria. (**B**) Characteristic responses of a 'regular spiking' pyramidal cell (upper trace) to hyperpolarizing and depolarizing current steps (lower trace) are shown. (**C**) Thirty minutes after establishing the whole-cell patch, glutamate (Glu, 300 μM) was applied, while monitoring cell membrane potential (current-clamp mode) and rhodamine-123 fluorescence in a neuron of AHS tissue. Glutamate elicited prolonged depolarization of the cell membrane and a train of action potentials (lower trace) that was followed by a transient elevation in rhodamine-123 fluorescence intensity in the cytosol (upper trace), indicating mitochondrial depolarization. The five images represent changes in cellular rhodamine-123 fluorescence (8-bit intensity calibration bar, right), whereas the trace illustrates changes in mean fluorescence intensity from a cytoplasmic region of interest.

explain smaller overshoots of NAD(P)H transients as compared to non-AHS tissue (Fig. 3B). At present, we cannot estimate the extent of impaired glial K^+-uptake that manifested itself during the range of neuronal activation as elicited in AHS tissue. Nevertheless, alterations of NAD(P)H transients were also observed in subiculum where impairment of glial K^+-uptake has not been found.

Negative mitochondrial membrane potential

The cell-permeable, cationic fluorescent dye, rhodamine-123 has been successfully used to monitor mitochondrial responses in a variety of preparations (Bindokas *et al.*, 1998; Ward *et al.*, 2000; Kovács *et al.*, 2002). Applying pharmacology and mitochondria-specific probes (Mito-Tracker®), we have further confirmed that rhodamine-123 is a specific and reliable tool for investigations on mitochondria (Schuchmann *et al.*, 2000; Kovács *et al.*, 2005).

Despite significant alterations in NAD(P)H transients in area CA1 from chronic epileptic rats and humans, rhodamine-123 accumulated in mitochondria of bulk-loaded slices and of patched neurons (Figs 4 and 5). Moreover, application of glutamate and CCCP elicited dye release to the cytoplasm in a similar range as compared to controls (Fig. 4) and to individual neurons in non-epileptic tissue (Kovács *et al.*, 2005). Because activity-dependent release of rhodamine-123 from mitochondria is commonly considered as reflecting mitochondrial depolarization during increased mitochondrial Ca^{2+}-uptake (Bindokas *et al.*, 1998;

Ward *et al.*, 2000), our data indicate that mitochondria in chronic epileptic tissue maintained a negative $\Delta\Psi_m$. In addition to mitochondrial Ca^{2+}-uptake, this would allow substrate transport across the inner mitochondrial membrane, and these mechanisms, in concert with mitochondrial enzyme activities, are key determinants in the regulation of $NAD(P)^+$ reduction and ATP generation (McCormack *et al.* 1990; Hansford and Zorov, 1998).

Metabolic dysfunction during neuronal activation

In pilocarpine-treated rats, we found unaltered drops but significantly smaller overshoots of NAD(P)H transients reflecting less effective $NAD(P)^+$ reduction (Fig. 3A). This difference was unlikely to be on account of less neuronal activation in chronic epileptic tissue, because increases in $[K^+]_o$ were virtually the same. Moreover, the difference was restricted to area CA1, which probably excluded an unspecific effect of pilocarpine treatment on metabolic functions in the animal model. Our findings are in line with observations that area CA1 is much more vulnerable to seizure-induced neuronal damage than the subiculum (Babb *et al.*, 1984; Mello *et al.*, 1993), and with the few reports that have described alterations of NAD(P)H transients in models of experimental epilepsy (Kunz *et al.*, 1999; Kovács *et al.*, 2002). In AHS and non-AHS tissue from TLE patients, we found very small overshoots of NAD(P)H transients (Fig. 3B). Together with the animal model data, we believe that this alteration is more a characteristic of the chronic epileptic human brain than of the human brain *per se*. At present, we cannot precisely determine whether the pronounced drops of NAD(P)H transients in human tissue exclusively reflect more severe alterations of $NAD(P)^+$ reduction and/or pathological variances in NAD(P)H oxidation and/or neuronal volume regulation. Though employing strategies of containment (Methods section), we cannot rule out the possibility that factors like antiepileptic drugs, anaesthesia and, potentially, tissue hypoxia during neurosurgery might have partially contributed to this phenomenon in human tissue (Gao *et al.*, 1995; Schuchmann *et al.*, 2001). In contrast to pilocarpine-treated rats, we observed no significant differences in alterations of NAD(P)H transients in both area CA1 and the subiculum when comparing AHS and non-AHS tissues. This deviant finding might be explained by prolonged disease duration in TLE patients (Table 1) and might indicate a gradual as well as spatial progression of metabolic dysfunction that becomes independent of the degree of sclerosis at later stages of TLE. This view is supported by neuroimaging studies also revealing 'hypometabolism' in brain structures adjacent to epileptic foci in patients (Casse *et al.*, 2002). Conversely, our data support the hypothesis that 'hypometabolism' is more a reflection of dysfunction in cellular energy metabolism than neuronal cell loss (see also Henry *et al.*, 1994; O'Brien *et al.*, 1997).

NAD(P)H fluorescence in living cells is a summation of cellular NAD(P)H oxidation and $NAD(P)^+$ reduction (Aubin, 1979; Schuchmann *et al.*, 2001). NAD(P)H oxidation reflects, e.g. enhanced cytochrome *c* oxidase activity upon a decrease in ATP/ADP ratio (Kadenbach, 2003) and/or enhanced mitochondrial generation of superoxide (Dringen, 2000; Nicholls, 2002) during neuronal activation. $NAD(P)^+$ reduction reflects enhanced activity of enzymes of the Krebs–Szentgyörgyi cycle in mitochondria as well as cytosolic glycolysis (Lipton, 1973; Duchen, 1992; Schuchmann, 2001). Thus, characteristic biphasic NAD(P)H fluorescence transients occur during neuronal activation in brain slice preparations (Fig. 2A), irrespective of the mode of stimulation (Kann *et al.*, 2003*a*, *b*; Shuttleworth *et al.*, 2003). Only recently, it has been proposed that the initial drop of NAD(P)H transients originates from the neuronal compartment whereas the prolonged overshoot is primarily astrocytic (Kasischke *et al.*, 2004). Nevertheless, biphasic NAD(P)H transients were described in individual sensory and hippocampal neurons (Duchen, 1992; Schuchmann *et al.*, 1998) similar to other cell types (Pralong *et al.*, 1994; Hajnóczky *et al.*, 1995; Robb-Gaspers *et al.*, 1998). These findings basically offer two intriguing options for interpreting our data from chronic epileptic tissue: firstly, there may be defects on the mitochondrial enzyme level in neurons (see also, Kunz *et al.*, 2000; Kudin *et al.*, 2002; Cock *et al.*, 2002) because small overshoots primarily reflect less effective mitochondrial $NAD(P)^+$ reduction, which are presumably not governed by collapsed $\Delta\Psi_m$ and mitochondrial Ca^{2+}-cycling (Figs 3–5) or decreased numbers of mitochondria (Blümcke *et al.*, 1999). Secondly, there may be a severe dysfunction on the level of astrocytic glycolysis and/or neuronal-astrocytic metabolic coupling (Magistretti and Pellerin, 1999; Kasischke *et al.*, 2004). At present, we cannot estimate the extent to which each of these mechanisms contributes to metabolic dysfunction during neuronal activation in chronic epileptic tissue.

Implications for temporal lobe epilepsy

Besides the central role in energy metabolism, NAD(P)H is a key element in a variety of intracellular signalling cascades (Berger *et al.*, 2004) and, e.g. essential for biosynthesis and reduction of cellular antioxidant, glutathione (Dringen, 2000; Nicholls, 2002). Thus, metabolic dysfunction in neurones and glial cells might significantly affect ATP homeostasis and excitability as well as intrinsic anti-oxidative mechanisms. Under certain conditions, these disturbances might favour neuronal vulnerability and manifestation of seizures and status epilepticus. Future epilepsy research might focus on alterations of intracellular signalling cascades and free radical generation during neuronal activation in chronic epileptic tissue, including their role in secondary tissue damage, as well as on effects of antiepileptic drugs on energy metabolism. Development of pharmacological tools for protection of mitochondria and free radical scavenging might serve as adjuvant therapy.

Acknowledgements

This study was supported by grants, ICA CT 2002 70007 (European Union), OTKA-F043589 (Hungary), Graduiertenkolleg 238, Sonderforschungsbereiche TR3 and 507 (Germany). The authors thank Drs K. Schulze, H. Siegmund and H.-J. Gabriel for excellent technical support, Drs K. Buchheim, S. Schuchmann, A. Friedman and M. J. Gutnick for very helpful discussions.

References

Ames A III. CNS energy metabolism as related to function. Brain Res Brain Res Rev 2000; 34: 42–68.

Aubin JE. Autofluorescence of viable cultured mammalian cells. J Histochem Cytochem 1979; 27: 36–43.

Avanzini G, Franceschetti S. Cellular biology of epileptogenesis. Lancet Neurol 2003; 2: 33–42.

Babb TL, Brown WJ, Pretorius J, Davenport C, Lieb JP, Crandall PH. Temporal lobe volumetric cell densities in temporal lobe epilepsy. Epilepsia 1984; 25: 729–40.

Berger F, Ramirez-Hernandez MH, Ziegler M. The new life of a centenarian: signalling functions of NAD(P). Trends Biochem Sci 2004; 29: 111–18.

Bindokas VP, Lee CC, Colmers WF, Miller RJ. Changes in mitochondrial function resulting from synaptic activity in the rat hippocampal slice. J Neurosci 1998; 18: 4570–87.

Blümcke I, Beck H, Lie AA, Wiestler OD. Molecular neuropathology of human mesial temporal lobe epilepsy. Epilepsy Res 1999; 36: 205–23.

Bruce JI, Giovannucci DR, Blinder G, Shuttleworth TJ, Yule DI. Modulation of $[Ca^{2+}]_i$ signaling dynamics and metabolism by perinuclear mitochondria in mouse parotid acinar cells. J Biol Chem 2004; 279: 12909–17.

Casse R, Rowe CC, Newton M, Berlangieri SU, Scott AM. Positron emission tomography and epilepsy. Mol Imaging Biol 2002; 4: 338–51.

Cavalheiro EA, Leite JP, Bortolotto ZA, Turski WA, Ikonomidou C, Turski L. Long-term effects of pilocarpine in rats: structural damage of the brain triggers kindling and spontaneous recurrent seizures. Epilepsia 1991; 32: 778–82.

Cock HR, Tong X, Hargreaves IP, Heales SJ, Clark JB, Patsalos PN et al. Mitochondrial dysfunction associated with neuronal death following status epilepticus in rat. Epilepsy Res 2002; 48: 157–68.

Dringen R. Metabolism and functions of glutathione in brain. Prog Neurobiol 2000; 62: 649–71.

Du F, Eid T, Lothman EW, Kohler C, Schwarcz R. Preferential neuronal loss in layer III of the medial entorhinal cortex in rat models of temporal lobe epilepsy. J Neurosci 1995; 15: 6301–13.

Duchen MR. Ca^{2+}-dependent changes in the mitochondrial energetics in single dissociated mouse sensory neurons. Biochem J 1992; 283: 41–50.

Engel J Jr. Mesial temporal lobe epilepsy: what have we learned? Neuroscientist 2001; 7: 340–52.

European Federation of Neurological Societies Task Force. Pre-surgical evaluation for epilepsy surgery—European standards. Eur J Neurol 2000; 7: 119–22.

Gabriel S, Njunting M, Pomper JK, Merschhemke M, Sanabria ER, Eilers A, et al. Stimulus and potassium-induced epileptiform activity in the human dentate gyrus from patients with and without hippocampal sclerosis. J Neurosci 2004; 24: 10416–30.

Gao XM, Margolis RL, Leeds P, Hough C, Post RM, Chuang DM. Carbamazepine induction of apoptosis in cultured cerebellar neurons: effects of N-methyl-D-aspartate, aurintricarboxylic acid and cycloheximide. Brain Res 1995; 703: 63–71.

Hajnóczky G, Robb-Gaspers LD, Seitz MB, Thomas AP. Decoding of cytosolic calcium oscillations in the mitochondria. Cell 1995; 82: 415–24.

Hansford RG, Zorov D. Role of mitochondrial calcium transport in the control of substrate oxidation. Mol Cell Biochem 1998; 184: 359–69.

Heinemann U, Arens, J. Production and calibration of ion-sensitive microelectrodes. In: Kettenmann H, Grantyn R, editors. Practical electrophysiological methods. New York: Wiley-Liss; 1992. p. 206–12.

Heinemann U, Lux HD. Undershoots following stimulus-induced rises of extracellular potassium concentration in cerebral cortex of cat. Brain Res 1975; 93: 63–76.

Heinemann U, Schaible HG, Schmidt RF. Changes in extracellular potassium concentration in cat spinal cord in response to innocuous and noxious stimulation of legs with healthy and inflamed knee joints. Exp Brain Res 1990; 79: 283–92.

Henry TR, Babb TL, Engel J Jr, Mazziotta JC, Phelps ME, Crandall PH. Hippocampal neuronal loss and regional hypometabolism in temporal lobe epilepsy. Ann Neurol 1994; 36: 925–27.

Hinterkeuser S, Schröder W, Hager G, Seifert G, Blümcke I, Elger CE, et al. Astrocytes in the hippocampus of patients with temporal lobe epilepsy display changes in potassium conductances. Eur J Neurosci 2000; 12: 2087–96.

Jackson JB. Proton translocation by transhydrogenase. FEBS Lett 2003; 545: 18–24.

Kadenbach B. Intrinsic and extrinsic uncoupling of oxidative phosphorylation. Biochim Biophys Acta 2003; 1604: 77–94.

Kann O, Schuchmann S, Buchheim K, Heinemann U. Coupling of neuronal activity and mitochondrial metabolism as revealed by NAD(P)H fluorescence signals in organotypic hippocampal slice cultures of the rat. Neuroscience 2003a; 119: 87–100.

Kann O, Kovács R, Heinemann U. Metabotropic receptor-mediated Ca^{2+} signaling elevates mitochondrial Ca^{2+} and stimulates oxidative metabolism in hippocampal slice cultures. J Neurophysiol 2003b; 90: 613–21.

Kasischke KA, Vishwasrao HD, Fisher PJ, Zipfel WR, Webb WW. Neural activity triggers neuronal oxidative metabolism followed by astrocytic glycolysis. Science 2004; 305: 99–103.

Kivi A, Lehmann TN, Kovacs R, Eilers A, Jauch R, Meencke HJ, et al. Effects of barium on stimulus-induced rises of $[K^+]_o$ in human epileptic non-sclerotic and sclerotic hippocampal area CA1. Eur J Neurosci 2000; 12: 2039–48.

Kovács R, Schuchmann S, Gabriel S, Kann O, Kardos J, Heinemann U. Free radical-mediated cell damage after experimental status epilepticus in hippocampal slice cultures. J Neurophysiol 2002; 88: 2909–18.

Kovács R, Kardos J, Heinemann U, Kann O. Mitochondrial calcium ion and membrane potential transients follow the pattern of epileptiform discharges in hippocampal slice cultures. J Neurosci 2005; 25: 4260–9.

Kudin AP, Kudina TA, Seyfried J, Vielhaber S, Beck H, Elger CE, et al. Seizure-dependent modulation of mitochondrial oxidative phosphorylation in rat hippocampus. Eur J Neurosci 2002; 15: 1105–14.

Kuhl DE, Engel J Jr, Phelps ME, Selin C. Epileptic patterns of local cerebral metabolism and perfusion in humans determined by emission computed tomography of 18FDG and 13NH3. Ann Neurol 1980; 8: 348–60.

Kunz WS, Goussakov IV, Beck H, Elger CE. Altered mitochondrial oxidative phosphorylation in hippocampal slices of kainate-treated rats. Brain Res 1999; 826: 236–42.

Kunz WS, Kudin AP, Vielhaber S, Blümcke I, Zuschratter W, Schramm J, et al. Mitochondrial complex I deficiency in the epileptic focus of patients with temporal lobe epilepsy. Ann Neurol 2000; 48: 766–73.

Lewis DV, Schuette WH. NADH fluorescence and $[K^+]_o$ changes during hippocampal electrical stimulation. J Neurophysiol 1975; 38: 405–17.

Lehmann TN, Gabriel S, Eilers A, Njunting M, Kovacs R, Schulze K, et al. Fluorescent tracer in pilocarpine-treated rats shows widespread aberrant hippocampal neuronal connectivity. Eur J Neurosci 2001; 14: 83–95.

Lipton P. Effects of membrane depolarization on nicotinamide nucleotide fluorescence in brain slices. Biochem J 1973; 136: 999–1009.

Magistretti PJ, Pellerin L. Cellular mechanisms of brain energy metabolism and their relevance to functional brain imaging. Philos Trans R Soc Lond B Biol Sci 1999; 354: 1155–63.

Margerison JH, Corsellis JA. Epilepsy and the temporal lobes. A clinical, electroencephalographic and neuropathological study of the brain in epilepsy, with particular reference to the temporal lobes. Brain 1966; 89: 499–530.

McCormack JG, Halestrap AP, Denton RM. Role of calcium ions in regulation of mammalian intramitochondrial metabolism. Physiol Rev 1990; 70: 391–425.

Mello LE, Cavalheiro EA, Tan AM, Kupfer WR, Pretorius JK, Babb TL, et al. Circuit mechanisms of seizures in the pilocarpine model of chronic epilepsy: cell loss and mossy fiber sprouting. Epilepsia 1993; 34: 985–95.

Nicholls DG. Mitochondrial function and dysfunction in the cell: its relevance to aging and aging-related disease. Int J Biochem Cell Biol 2002; 34: 1372–81.

Nicholls DG, Budd SL. Mitochondria and neuronal survival. Physiol Rev 2000; 80: 315–60.

O'Brien TJ, Newton MR, Cook MJ, Berlangieri SU, Kilpatrick C, Morris K et al. Hippocampal atrophy is not a major determinant of regional hypometabolism in temporal lobe epilepsy. Epilepsia 1997; 38: 74–80.

Parent JM, Lowenstein DH. Mossy fiber reorganization in the epileptic hippocampus. Curr Opin Neurol 1997; 10: 103–9.

Pitkänen A, Sutula TP. Is epilepsy a progressive disorder? Prospects for new therapeutic approaches in temporal-lobe epilepsy. Lancet Neurol 2002; 1: 173–81.

Pralong WF, Spät A, Wollheim CB. Dynamic pacing of cell metabolism by intracellular Ca^{2+} transients. J Biol Chem 1994; 269: 27310–14.

Racine RJ. Modification of seizure activity by electrical stimulation. II. Motor seizure. Electroencephalogr Clin Neurophysiol 1972; 32: 281–94.

Robb-Gaspers LD, Burnett P, Rutter GA, Denton RM, Rizzuto R, Thomas AP. Integrating cytosolic calcium signals into mitochondrial metabolic responses. EMBO J 1998; 17: 4987–5000.

Schuchmann S, Müller W, Heinemann U. Altered Ca^{2+} signaling and mitochondrial deficiencies in hippocampal neurons of trisomy 16 mice: a model of Down's syndrome. J Neurosci 1998; 18: 7216–31.

Schuchmann S, Lückermann M, Kulik A, Heinemann U, Ballanyi K. Ca^{2+}- and metabolism-related changes of mitochondrial potential in voltage-clamped CA1 pyramidal neurons in situ. J Neurophysiol 2000; 83: 1710–21.

Schuchmann S, Kovács R, Kann O, Heinemann U, Buchheim K. Monitoring NAD(P)H autofluorescence to assess mitochondrial metabolic functions in rat hippocampal-entorhinal cortex slices. Brain Res Brain Res Protoc 2001; 7: 267–76.

Shuttleworth CW, Brennan AM, Connor JA. NAD(P)H fluorescence imaging of postsynaptic neuronal activation in murine hippocampal slices. J Neurosci 2003; 23: 3196–208.

Somjen GG. Electrophysiology of mammalian glial cells in situ. In: Kettenmann H, Ransom BR, editors. Neuroglia. Oxford: Oxford University Press; 1995. p. 319–31.

Steinhäuser C, Seifert G. Glial membrane channels and receptors in epilepsy: impact for generation and spread of seizure activity. Eur J Pharmacol 2002; 447: 227–37.

Sutula T, Cascino G, Cavazos J, Parada I, Ramirez L. Mossy fiber synaptic reorganization in the epileptic human temporal lobe. Ann Neurol 1989; 26: 321–30.

Ward MW, Rego AC, Frenguelli BG, Nicholls DG. Mitochondrial membrane potential and glutamate excitotoxicity in cultured cerebellar granule cells. J Neurosci 2000; 20: 7208–19.

Wyler AR, Dohan Jr FC, Schweitzer JB, Berry AD. A grading system for mesial temporal pathology (hippocampal sclerosis) from anterior temporal obectomy. J Epilepsy 1992; 5: 220–5.